Ferroelectricity in Lu doped HfO_2 layers

T. C. U. Tromm, J. Zhang, J. Schubert, M. Luysberg, W. Zander, Q. Han, P. Meuffels, D. Meertens, S. Glass, P. Bernardy, and S. Mantl

Citation: Appl. Phys. Lett. **111**, 142904 (2017); doi: 10.1063/1.4998336
View online: http://dx.doi.org/10.1063/1.4998336
View Table of Contents: http://aip.scitation.org/toc/apl/111/14
Published by the American Institute of Physics

Ferroelectricity in Lu doped HfO_2 layers

T. C. U. Tromm,[1] J. Zhang,[1] J. Schubert,[1] M. Luysberg,[2] W. Zander,[1] Q. Han,[1] P. Meuffels,[3] D. Meertens,[2] S. Glass,[1] P. Bernardy,[1] and S. Mantl[1]
[1]*Peter-Grünberg-Institut (PGI 9 IT), Forschungszentrum Jülich GmbH, Jülich 52428, Germany and JARA, Fundamentals of Future Information Technology, Jülich 52425, Germany*
[2]*Ernst Ruska Centrum 1, Forschungszentrum Jülich GmbH, Jülich 52428, Germany*
[3]*Peter-Grünberg-Institut (PGI 7), Forschungszentrum Jülich GmbH, Jülich 52428, Germany and JARA, Fundamentals of Future Information Technology, Jülich, Germany*

(Received 31 July 2017; accepted 23 September 2017; published online 3 October 2017)

Doped HfO_2 has become a promising candidate for non-volatile memory devices since it can be easily integrated into existing CMOS technology. Many dopants like Y, Gd, and Sr have been investigated for the stabilization of ferroelectric HfO_2. Here, we report the fabrication of capacitors comprising ferroelectric HfO_2 metal-insulator-metal structures with TiN bottom and top electrodes using the dopant Lu. Amorphous 5% Lu doped HfO_2 was deposited by pulsed laser deposition and afterwards annealed to achieve the ferroelectric, orthorhombic phase (space group $Pbc2_1$). The polarization of the layers was confirmed by capacitance-voltage, polarization-voltage, and current-voltage measurements. Depending on the anneal temperature, the remanent polarization changes and the initial state of the oxide varies. The layer exhibits initially a pinched hysteresis up to an annealing temperature of 600 °C and an unpinched hysteresis at 700 °C. The maximum polarization is about 11 $\mu C/cm^2$ which is measured after 10^4 cycles and stable up to 10^6 cycles. The influence of the layer thickness on the oxide properties is investigated for 10–40 nm thick HfLuO; however, a thickness dependence of the ferroelectric properties is not observed. *Published by AIP Publishing.*
https://doi.org/10.1063/1.4998336

HfO_2 is commonly used as a high-κ dielectric in state-of-the-art complementary metal-oxide-semiconductor devices. HfO_2 layers are usually grown in the amorphous phase and can be crystallized during a rapid thermal anneal. In recent years, ferroelectric properties have been discovered in polycrystalline HfO_2 layers doped with Y,[1] Sr,[2] Gd,[3] Zr,[4] Al,[5] and Si,[6] which is ascribed to the metastable, non-centrosymmetric, orthorhombic phase ($Pbc2_1$)[7] being stabilized by the dopants. While common ferroelectrics like lead zirconate titanate are difficult to integrate into the existing CMOS technology,[8] doped HfO_2 can overcome this disadvantage. Thus, doped HfO_2 is an attractive ferroelectric candidate for ferroelectric random access memories[9] or negative capacitance field effect transistors.[10]

In this work, we investigated the properties of 5% Lu doped HfO_2 (HfLuO) layers. The layers were deposited by pulsed laser deposition (PLD)[11] which offers a stoichiometric deposition of the layer. For electrical characterization, metal-insulator-metal (MIM) structures with TiN top and bottom electrodes were grown and investigated by polarization-voltage (PV), current-voltage (IV), and capacitance-voltage (CV) measurements.

Planar $20 \times 20\,mm^2$ MIM structures were fabricated. 8 in. Si wafers were RCA cleaned before 40 nm TiN was deposited as the bottom electrode by reactive sputtering. The wafers were cut into $20 \times 20\,mm^2$ pieces and cleaned with acetone and isopropanol before depositing the ferroelectric layer. The HfLuO layers were grown by PLD using a KrF excimer laser (pulse width: 20 ns, fluence of 2.5 J cm^{-2}, and wavelength: 248 nm) at room temperature. The target for deposition was prepared using hafnium oxide (HfO_2, 99.9%) and lutetium oxide (Lu_2O_3, 99.9%) powders. Appropriate amounts of the powders were mixed together and ground by ball milling using zirconia grinding balls. Thereafter, cylindrical green bodies 22 mm in diameter and 7 mm in height were formed by cold isostatic pressing at 800 MPa. Before pressing, the powder mixture was granulated by adding a binder to enhance the fracture strength of the green bodies. The binder was burnt off before sintering by firing at 600 °C for 12 h in air. Sintering was performed at 1600 °C for 8 h in air. The layer thickness varied from 10 to 40 nm.

After deposition of the HfLuO layer, a 40 nm TiN top electrode was sputtered and 50 nm Pt contacts were deposited by electron beam evaporation via a shadow mask. The samples were annealed at temperatures between 400 and 700 °C for 30 s in Ar using a Mattson Helios. The TiN in between the Pt pads was etched by reactive ion etching and SC1 at room temperature after annealing. For electrical characterization, two top contacts with an area ratio of 400 ($4\,mm^2$:$0.01\,mm^2$) were contacted. Since capacitors connected in series are added reciprocally, the measured capacitance is approximately equal to the capacity of the small pad. The samples were investigated by PV using an aixACCT TF 2000 and by CV and IV using an Agilent E4980A precision LCR meter. The CV measurements were performed at a frequency of 100 kHz and with a 50 mV ac probing signal. The layer thickness was determined from x-ray reflectivity, and the structure was measured by grazing incidence x-ray diffraction (GIXRD). The FIB lamella was prepared using a Helios NanoLab 400S. Before cutting, an Au layer was sputtered on top. The lamella was cut at 30 keV and polished at 5 keV. A Fischione NanoMill Model 1040 was used for further ion milling and surface cleaning the lamella at 900 eV and 500 eV by Argon, respectively. The structures were investigated by transmission electron microscopy (TEM) with FEI Tecnai G2 F20[12] operated at 200 kV.

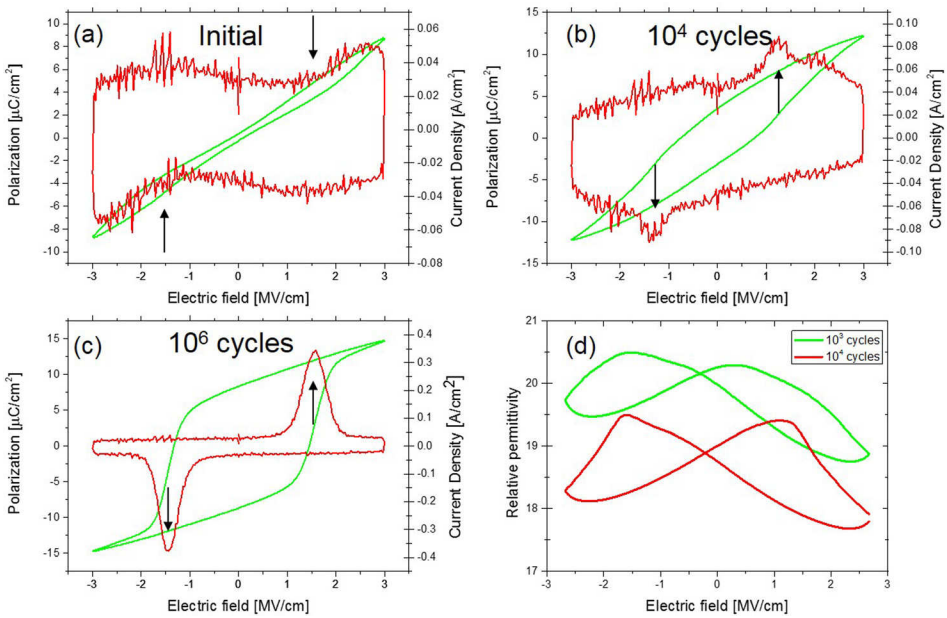

FIG. 1. PV measurement (green line) and current density (red line) of the TiN/30 nm $HfLuO_2$/TiN/Pt sample annealed at 500 °C in the initial state (a), after 10^4 cycles (b), and after 10^6 cycles (c). The polarization increases by cycling and P_r of 8.4 $\mu C/cm^2$ and $-8.7\ \mu C/cm^2$ is determined. Arrows indicate the position of increasing current due to domain switching. (d) The permittivity calculated from the CV measurement shows the characteristic peaks and decreases during cycling.

Ferroelectric properties have been investigated by measurements of polarization and capacitance. In particular, the influence of the annealing temperature on the ferroelectric properties has been studied. Figure 1 shows the PV measurement of a 30 nm layer HfLuO annealed at 500 °C. The hysteresis of the initial state is pinched indicating the existence of an antiferroelectric phase or other defects like domain wall pinning[13] [see Fig. 1(a)]. After 10^4 cycles, the sample becomes ferroelectric [see Fig. 1(b)] and the polarization increases up to 10^6 cycles [see Fig. 1(c)]. The remanent polarization (P_r) of the layer after 10^6 cycles is 8 $\mu C/cm^2$ and $-9\ \mu C/cm^2$. The determined P_r is lower compared to other PLD grown ferroelectric HfO_2 like $HfYO_2$ (13 $\mu C/cm^2$)[14] and $HfGdO_2$ (12 $\mu C/cm^2$).[15] In the IV curve [s. Figs. 1(a)–1(c) red line], the so called "wake-up" of the ferroelectric domains is visible by the increasing current density. While at the initial state of the ferroelectric layer no increase in the current density is visible at an electric field of 1.6 MV/cm and −1.5 MV/cm, the current density increases after 10^6 cycles up to -0.38 A/cm^2 and 0.35 A/cm^2. This is related to the switching of the ferroelectric domains resulting in a detectable current. From CV measurements, the permittivity (κ) was calculated showing two characteristic peaks, which reach a maximum value of 20.5 [see Fig. 1(d)]. The permittivity is much lower compared to PLD deposited $HfYO_2$[14] (40) and PLD deposited $HfGdO_2$[15] (50). The reason for the lower permittivity could be an interfacial layer or a mixture of the ferroelectric phase and a low κ phase. Further cycling of the oxide decreases the permittivity, which has been reported for other PLD deposited layers,[14] too. The initial state is stabilized in a temperature range from 400 to 600 °C. An initial stable hysteresis is favorable for any application to keep the layer properties stable during operating life. Therefore, higher annealing temperatures were tested.

Figure 2(a) shows the characteristic PV measurement of a 30 nm HfLuO layer annealed at 700 °C with initial P_r values of 5 $\mu C/cm^2$ and $-4\ \mu C/cm^2$ and E_C values of 0.6 MV/cm^2 and -0.8 MV/cm^2. Further "wake-up" cycles are needed to reach the maximum polarization of up to 11 $\mu C/cm^2$ and $-10\ \mu C/cm^2$, which is comparable to other PLD grown ferroelectric HfO_2.[14,15] After 10^4 cycles, the maximum polarization is reached and does not increase with further cycling. From the measured CV curve, the relative permittivity is calculated [Fig. 2(b)] exhibiting the characteristic butterfly shape. The calculated permittivity is about 22.5 after 10^3 cycles, which is slightly higher compared to the layers annealed at 500 °C. After 10^4 cycles, the permittivity is reduced, too. The influence of the layer thickness on the oxide properties is investigated for 10–40 nm thick HfLuO. In contrast to ALD grown layers, the PLD grown HfLuO layers show no thickness dependence of the polarization. This results from the deposition at room temperature other than for ALD deposited layers, which crystallize during growth, because of the higher process temperature.

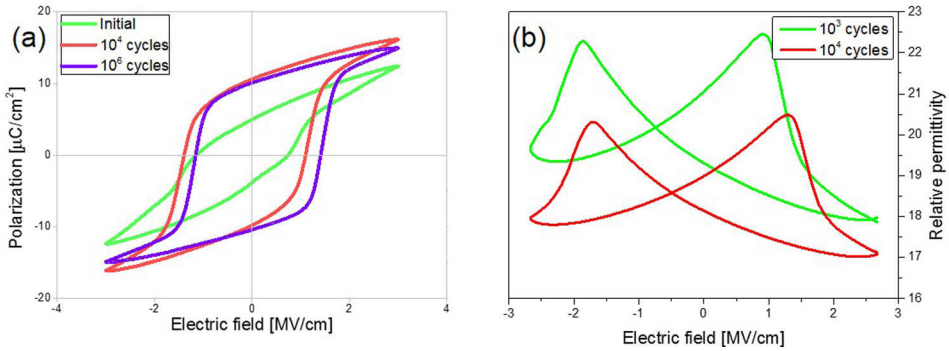

FIG. 2. (a) PV measurement of TiN/30 nm $HfLuO_2$/TiN/Pt sample annealed at 700 °C. The sample is initially ferroelectric, while further cycling up to 10^4 cycles increases the polarization up to 11 $\mu C/cm^2$ and $-10\ \mu C/cm^2$. The E_c is 0.6 MV/cm^2 and 0.8 MV/cm^2. (b) The permittivity calculated from the CV measurement shows the characteristic peaks and decreases during cycling.

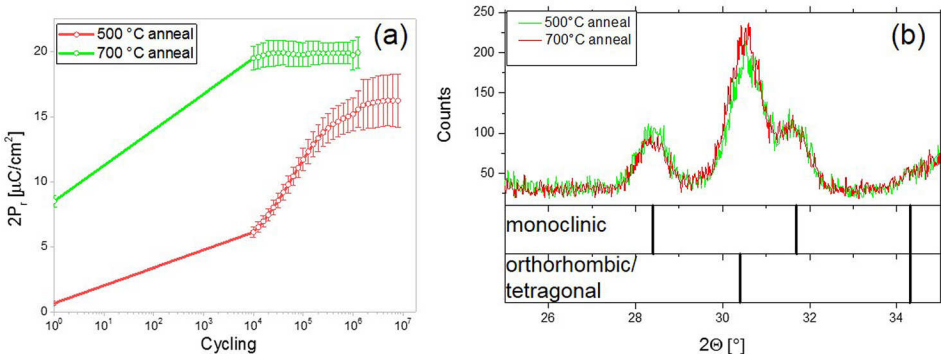

FIG. 3. Comparison of the samples annealed at 500 °C and 700 °C. (a) Fatigue measurement shows a higher polarization of the 700 °C sample and fewer cycles before breakdown. Both samples show no decrease in polarization before breakdown. (b) GIXRD exhibits for both samples monoclinic and orthorhombic/tetragonal peaks with comparable ratio.

Annealing temperatures larger than 700 °C cause increased leakage current.

A further important characteristic of a ferroelectric layer is the fatigue phenomena, which describes the change of the polarization by cycling. Figure 3(a) shows the fatigue measurement of the 500 °C and 700 °C samples at an electric field of 3 MV/cm, whereby the polarization is the sum of the absolute values of the positive and the negative P_r. The sample annealed at 700 °C reaches the maximum polarization after 10^4 cycles, while the sample annealed at 500 °C attains the maximum polarization after 10^6 cycles. The assumed reason for the "wake-up" effect of HfO_2 is the redistribution of oxygen vacancies and a phase change in the layer.[16,17] At the initial state, the oxygen vacancies are distributed inhomogeneous at the grain boundaries of the HfO_2.[18] Therefore, some domains are pinned by the oxygen vacancies, so that they do not switch at the initial state and do not contribute to the measured P_r. By cycling, the oxygen vacancies are redistributed, so that the domain wall pinning is abolished and more domains are switched by the applied field resulting in an increased polarization. Furthermore, the oxygen vacancy redistribution supports a phase transformation of the monoclinic and tetragonal phase to the ferroelectric orthorhombic phase increasing P_r. The longer "wake-up" effect of the 500 °C samples could be related to a more inhomogeneous distribution of the oxygen vacancies compared to the layer annealed at 700 °C. Furthermore, the 700 °C sample breaks down after 10^6 cycles, while the 500 °C sample endures up to 10^7 cycles.[14] Both samples show no reduction of P_r before breakdown. PLD grown $HfYO_2$ achieves a comparable amount of cycles (10^7) and no P_r reduction before breakdown at the maximum polarization.[14] Figure 3(b) shows the GIXRD of both samples exhibiting two peaks at 28.4° and 31.7°, which can be assigned to the monoclinic phase. Since monoclinic HfO_2 is known to exhibit only a permittivity of 20,[19] compared to other ferroelectric layers ($\kappa \sim 40$),[14] the reduced permittivity can be explained by the presence of the monoclinic phase. Furthermore, a peak at 30.4° is visible, which indicates the existence of the orthorhombic/tetragonal phase, which cannot be distinguished due to the similar lattice parameters. Since the ratio of the monoclinic and the orthorhombic/tetragonal peaks is comparable, the different initial behavior of the sample annealed at 500 °C can result from a higher tetragonal ratio, which is assumed to be the antiferroelectric phase.[7]

TEM bright and dark field images shown in Fig. 4 reveal the structural properties of the Si/TiN/HfLuO/TiN stack. The bright field image in Fig. 4(a) displays the interfaces of the Si substrate to the TiN layer, which is covered by the HfLuO film showing darker contrast. In between the bottom electrode and the Si, an interfacial SiO_2 layer is visible, which can be identified by its bright contrast. The interface between the TiN and the HfLuO is seen to be rough. Individual crystalline grains within the TiN layer can be identified, one of them showing Moire fringes. To obtain the dark field image [Fig. 4(b)], an objective aperture was placed on the first ring of reflections as indicated by the circle in the inset, which displays the diffraction pattern. Areas of the investigated region, which scatter into the aperture, appear bright. Within the TiN layer, only small grains of approximately 10 nm in width are seen. Within the HfLuO layer, one single grain 82 nm in width is detected, which extends from the bottom to the top of the film.

Lu doping of HfO_2 causes the growth of the ferroelectric, orthorhombic phase. The P_r of 11 $\mu C/cm^2$ is comparable to other PLD grown, ferroelectric doped HfO_2 like $HfGdO_2$ (12 $\mu C/cm^2$) or $HfYO_2$ (15 $\mu C/cm^2$). The determined κ of 22.5 is significantly lower. The fatigue behavior of HfLuO at the maximum P_r (10^6) is one magnitude smaller compared to $HfYO_2$ (10^7). For further optimization, the fabrication needs to be optimized especially in respect of the Lu content. Nevertheless, 5%-Lu doped HfO_2 exhibits the potential to change the initial ferroelectric properties. Thus, the material offers a large number of possible applications, which can be fabricated using a constant dopant concentration. Antiferroelectric

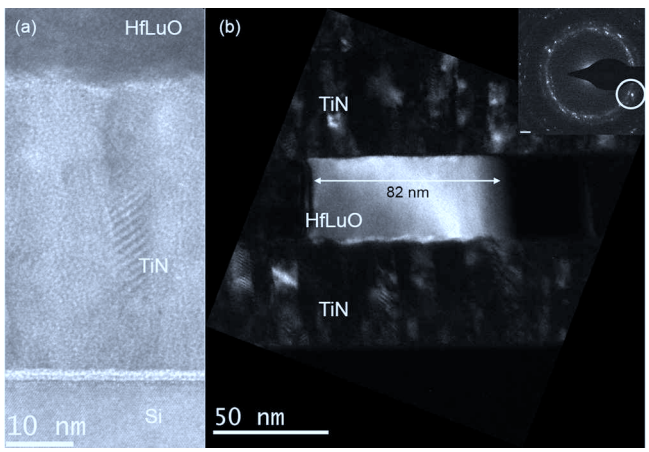

FIG. 4. TEM images of the TiN/30 nm $HfLuO_2$/TiN/Pt sample annealed at 700 °C. (a) Overview of the structure exhibiting a rough HfLuO/TiN interface. (b) DF image of the $HfLuO_2$ layer exhibiting grain sizes up to 82 nm in-plane.

HfLuO could be used for energy storage, infrared sensing for thermal imaging[7] or as a nonvolatile storage with a fixed internal bias field,[20] while ferroelectric HfLuO can be used for ferroelectric random access memories[9] or negative capacitance field effect transistors.[10] Further research will investigate the reason for the different initial properties and the cause for the pinched hysteresis.

In summary, we have fabricated MIM structures with TiN electrodes and 5%Lu-doped HfO_2. The Lu doping resulted in a stabilization of the ferroelectric phase. The initial oxide properties depend on the annealing temperature, resulting in a pinched hysteresis at 400–600 °C, showing ferroelectricity at 700 °C and increased leakage current at higher annealing temperatures. The pinched hysteresis could result from an initial antiferroelectric phase or other effects like domain wall pinning.[13] Thus, 5%-Lu doped HfO_2 offers a large variety of applications. Cycling of the layers annealed at 500 °C switches the pinned hysteresis to a ferroelectric behavior. HfLuO annealed at 700 °C achieves a P_r of 11 μC/cm^2 and shows stable polarization up to 10^6 cycles, while breakdown occurs suddenly without reduced polarization. All layers are partially monoclinic proven by GIXRD. The permittivity is about 22.5 and low compared to other ferroelectric layers due to a partially monoclinic oxide. TEM images of a sample annealed at 700 °C show a rough interface between the HfLuO and the TiN. Furthermore, the layer is completely crystallized and exhibits grains up to 82 nm width.

The authors thank the German-Israeli Foundation for Scientific Research and Development for financial support of this Project (I-1273-401.10/2014).

[1]S. Starschich, D. Griesche, T. Schneller, R. Waser, and U. Böttger, Appl. Phys. Lett. **104**(20), 202903 (2014).
[2]U. Schroeder, E. Yurchuk, J. Müller, D. Martin, T. Schenk, P. Polakowski, C. Adelmann, M. I. Popovici, S. V. Kalinin, and T. Mikolajick, Jpn. J. Appl. Phys., Part 1 **53**(8S1), 08LE02 (2014).
[3]S. Mueller, C. Adelmann, A. Singh, S. Van Elshocht, U. Schroeder, and T. Mikolajick, ECS J. Solid State Sci. Technol. **1**(6), N123 (2012).
[4]S. Zarubin, E. Suvorova, M. Spiridonov, D. Negrov, A. Chernikova, A. Markeev, and A. Zenkevich, Appl. Phys. Lett. **109**(19), 192903 (2016).
[5]S. Mueller, J. Mueller, A. Singh, S. Riedel, J. Sundqvist, U. Schroeder, and T. Mikolajick, Adv. Funct. Mater. **22**(11), 2412 (2012).
[6]P. D. Lomenzo, Q. Takmeel, C. Zhou, C. Chung, S. Moghaddam, J. L. Jones, and T. Nishida, Appl. Phys. Lett. **107**(24), 242903 (2015).
[7]M. H. Park, Y. H. Lee, H. J. Kim, Y. J. Kim, T. Moon, K. D. Kim, J. Muller, A. Kersch, U. Schroeder, T. Mikolajick, and C. S. Hwang, Adv. Mater. **27**(11), 1811 (2015).
[8]K. Kim and S. Lee, J. Appl. Phys. **100**(5), 051604 (2006).
[9]F. Huang, Y. Wang, X. Liang, J. Qin, Y. Zhang, X. Yuan, Z. Wang, B. Peng, L. Deng, Q. Liu, L. Bi, and M. Liu, IEEE Electron Device Lett. **38**(3), 330 (2017).
[10]M. H. Lee, P.-G. Chen, C. Liu, K.-Y. Chu, C.-C. Cheng, M.-J. Xie, S.-N. Liu, J.-W. Lee, S.-J. Huang, M.-H. Liao, M. Tang, K.-S. Li, and M.-C. Chen, *2015 IEEE International Electron Devices Meeting (IEDM)*, (Washington, DC, 2015), pp. 22.5.1–22.5.4.
[11]C. Buchal, L. Beckers, A. Eckau, J. Schubert, and W. Zander, Mater. Sci. Eng. B-Solid State Mater. Adv. Technol. **56**(2–3), 234 (1998).
[12]M. Luysberg, M. Heggen, and K. Tillmann, J. Large Scale Res. Facil. **2**, A77 (2016).
[13]T. Rojac, M. Kosec, B. Budic, N. Setter, and D. Damjanovic, J. Appl. Phys. **108**(7), 074107 (2010).
[14]F. Huang, Y. Wang, X. Liang, J. Qin, Y. Zhang, T. Huang, Z. Wang, B. Peng, P. Zhou, H. Lu, L. Zhang, L. Deng, M. Liu, Q. Liu, H. Tian, and L. Bi, Phys. Chem. Chem. Phys. **19**(5), 3486 (2017).
[15]Y. Sharma, D. Barrionuevo, R. Agarwal, S. P. Pavunny, and R. S. Katiyar, ECS Solid State Lett. **4**(11), N13 (2015).
[16]M. Pesic, F. P. G. Fengler, L. Larcher, A. Padovani, T. Schenk, E. D. Grimley, X. Sang, J. M. LeBeau, S. Slesazeck, U. Schroeder, and T. Mikolajick, Adv. Funct. Mater. **26**(25), 4601 (2016).
[17]U. Schroeder, M. Pešić, T. Schenk, H. Mulaosmanovic, S. Slesazeck, J. Ocker, C. Richter, E. Yurchuk, K. Khullar, J. Müller, P. Polakowski, E. D. Grimley, J. M. LeBeau, S. Flachowsky, S. Jansen, S. Kolodinski, R. van Bentum, A. Kersch, C. Künneth, and T. Mikolajick, in *2016 46th European Solid-State Device Research Conference (Essderc)* (2016), p. 364.
[18]T. Schenk, U. Schroeder, M. Pesic, M. Popovici, Y. V. Pershin, and T. Mikolajick, ACS Appl. Mater. Interfaces **6**(22), 19744 (2014).
[19]S. Kar, *High Permittivity Gate Dielectric Materials*, 1st ed. (Springer-Verlag Berlin Heidelberg, 2013).
[20]M. Pešić, S. Knebel, M. Hoffmann, C. Richter, T. Mikolajick, and U. Schroeder, in 2016 IEEE International Electron Devices Meeting (IEDM) (2016).